# Novel *CLCN7* mutations cause autosomal dominant osteopetrosis type II and intermediate autosomal recessive osteopetrosis

LI LI[*], SHAN-SHAN LV[*], CHUN WANG, HUA YUE and ZHEN-LIN ZHANG

Metabolic Bone Disease and Genetic Research Unit, Department of Osteoporosis and Bone Disease,
Shanghai Jiao Tong University Affiliated Sixth People's Hospital, Shanghai 200233, P.R. China

**Abstract.** Osteopetrosis refers to a group of rare genetic bone diseases that are clinically characterized by increased bone mass and fragility. The principal pathogenic defect in patients with chloride channel 7 (*CLCN7*) gene-dependent osteopetrosis is reduced osteoclast activity, which leads to decreased bone resorption. Mutations in the *CLCN7* gene result in autosomal dominant osteopetrosis type II (ADO-II), autosomal recessive osteopetrosis (ARO) and intermediate ARO (IARO). In the present study, eight mutations in the *CLCN7* gene were identified in six patients with familial osteopetrosis and one patient with sporadic osteopetrosis. Heterozygous mutations c.856C>T (R286W), c.2236T>G (Y746D), c.296A>G (Y99C) and c.937G>A (E313K), and a splice mutation (c.2232-2A>G) in the *CLCN7* gene were detected in patients with ADO-II. A homozygous mutation c.2377G>C (G793R), and a compound heterozygous mutation c.1409C>T (P470L) and c.647_648dupTG (K217X) were detected in two Chinese families with IARO. Among these mutations, two heterozygous mutations (c.2236T>G and c.2232-2A>G), one homozygous mutation (c.2377G>C) and the compound heterozygous mutation (c.1409C>T and c.647_648dupTG) are novel, to the best of our knowledge. The present findings not only broaden the allelic spectrum of *CLCN7* mutations, but also provide increased knowledge of the clinical phenotypes observed in Chinese patients with osteopetrosis.

*Correspondence to:* Professor Zhen-Lin Zhang or Professor Hua Yue, Metabolic Bone Disease and Genetic Research Unit, Department of Osteoporosis and Bone Disease, Shanghai Jiao Tong University Affiliated Sixth People's Hospital, 600 Yishan Road, Shanghai 200233, P.R. China
E-mail: zhangzl@sjtu.edu.cn
E-mail: yueyinglonghua@163.com

[*]Contributed equally

## Introduction

Osteopetrosis refers to a heterogeneous group of rare bone disorders characterized by reduced osteoclast activity (1-3), which results in increased bone mass and decreased bone strength. The disease is classified into three major clinical subtypes according to the severity and mode of inheritance: Autosomal recessive osteopetrosis (ARO); intermediate ARO (IARO); and autosomal dominant osteopetrosis (ADO) (4). Mutations in the chloride channel 7 (*CLCN7*) gene locus on chromosome 16p13.3 have been reported to cause ARO, IARO and ADO type II (ADO-II) (5,6). To date, all reported cases of ADO-II are associated with mutations in the *CLCN7* gene. The *CLCN7* gene encodes the 803-amino acid chloride channel protein 7 (ClC-7), which provides the chloride conductance necessary for efficient proton pumping in the osteoclast ruffled membrane (4) and is involved in acidification of the resorption lacuna. A low-pH microenvironment is required during normal bone resorption (1). Osteoclasts are multinucleated giant cells responsible for bone resorption, which serve important roles during bone growth and tissue renewal (7). With the balance of bone modeling and remodeling, the normal mineralized matrix erosion activity of osteoclasts serves to maintain healthy and mechanically competent bone (8). Conversely, dysfunctional osteoclasts lead to osteopetrosis. The majority of patients are diagnosed with ADO, with an incidence of ~1 per 20,000 individuals (2,9).

ADO-II (OMIM 166600; www.omim.org), also known as Albers-Schönberg disease or marble bone disease, is a form of ADO comprising a clinical spectrum ranging from very mild to severe disease phenotypes, with a reported penetrance of 56-90% in different studies (1,10). The range of phenotypes observed under the ADO-II spectrum includes asymptomatic disease, osteosclerosis, a high rate of fractures, osteomyelitis, and hematological and neural defects (2). IARO is a milder form of ARO; patients with IARO manifest mandibular prognathism, occasional osteomyelitis, hepatosplenomegaly and a tendency to develop fractures (4). Radiographs of affected individuals reveal diffuse osteosclerosis and pathognomonic findings of 'bone-within-bone' or 'endobones' due to parallel bands of dense bone, which are often prominent in the pelvis, vertebrae and long bones (11). The thickening of the end plate in the vertebrae is termed 'sandwich vertebrae' or 'rugger jersey spine'. Alterations in the metaphysis of long bones are termed 'Erlenmeyer flask bone deformities' (12,13).

At present, >23 mutations in *CLCN7* have been identified in Chinese families with ADO-II (11,14-20). Among them, 14 mutations were reported in our previous studies (10,14,16,20). A few cases of IARO in China have been reported by Xue *et al* (17), Pang *et al* (19) and Zhang *et al* (16). In the present study, the clinical and molecular characterization of another five patients with ADO-II and two patients with IARO were reported. Additionally, four novel mutations were identified.

**Materials and methods**

*Patients*. The present study was approved by the Ethics Committee of the Shanghai Jiao Tong University Affiliated Sixth People's Hospital. All subjects who participated in the study were recruited by the Department of Osteoporosis and Bone Disease of the Shanghai Jiao Tong University Affiliated Sixth People's Hospital between December 2016 and December 2018, and all signed informed consent documents prior to entering the project. A total of seven families were included. All subjects were of Han ethnicity and had non-consanguineous parents. The pedigrees of the families with ADO-II and IARO are presented in Fig. 1.

*Biochemical measurements*. Fasting peripheral blood samples were collected from each subject during a clinical visit and were analyzed in the central laboratory of Shanghai Jiao Tong University Affiliated Sixth People's Hospital. Full blood count, including haemoglobin and platelets, and phosphate, calcium, alkaline phosphatase (ALP), creatinine, alanine transaminase, aspartate transaminase, lactate dehydrogenase (LDH), creatine kinase (CK) and CK-MB levels were measured using a Hitachi 7600 automatic biochemical analyzer (Hitachi, Ltd., Tokyo, Japan). Serum parathyroid hormone (PTH) concentrations, and Serum 25-hydroxyvitamin D (25OHD) levels were measured using an ECLIA Elecsys autoanalyzer (E170; Roche Diagnostic GmbH, Mannheim, Germany).

*Measurement of radiographs and bone mineral density (BMD)*. Radiographic studies were performed at the Department of Radiology of Shanghai Jiao Tong University Affiliated Sixth People's Hospital. X-rays of the skull, thoracic and lumbar vertebrae, distal femoral and proximal tibiae, and pelvis were acquired to detect bone abnormalities.

The BMD (g/cm$^2$) of the lumbar spine (L1-4) and the left proximal femur, including the femoral neck and total hip, were measured using dual-energy X-ray absorptiometry densitometers at the Department of Osteoporosis and Bone Disease of Shanghai Jiao Tong University Affiliated Sixth People's Hospital.

*Molecular genetics analyses*. All fasting blood samples were collected in the morning for laboratory tests and DNA analyses. Genomic DNA was isolated from peripheral white blood cells from 2 ml blood using a DNA extraction kit (Shanghai Laifeng Biotechnology Co., Ltd., Shanghai, China; http://www.lifeng.com) according to the manufacturer's protocol. The *CLCN7* gene was screened for mutations in the probands from the seven families. A database was analysed and additional mutation sites were identified in other family members and 250 healthy ethnically matched controls (125 males and 125 females) (14). All 25 exons of the *CLCN7* gene, including the exon-intron boundaries, were amplified via polymerase chain reaction (PCR) using 16 pairs of primers: CLCN7E1 forward (F): 5'-CGACCG GGCCTCGGTGGTT-3', CLCN7E1 reverse (R): 5'-GCG GCCTCCGAAGACTCCAGACC-3', CLCN7E2 F: 5'-AGC CGGATCAGTTCTGCTT-3', CLCN7E2 R: 5'-CACTCC TCCGTCTGAGAGCA-3', CLCN7E3_4 F: 5'-CCCCAT GTGCAGTTCTCTTG-3', CLCN7E3_4 R: 5'-AGCAGC CTTCTTGGTTACGG-3', CLCN7E5_6 F: 5'-CACTGG GCCCTTCATAATCC-3', CLCN7E5_6 R: 5'-TTCTAA AAGTGCCCGGGTTG-3', CLCN7E7 F: 5'-GACGTGTGT GCTGCTCTTCC-3', CLCN7E7 R: 5'-CAAACTGAAAGC GGGAAACTG-3', CLCN7E8_9 F: 5'-CCCAGCCACTCT GCCTGATC-3', CLCN7E8_9 R: 5'-CGCCAGGCTGTC CTCAGAT-3', CLCN7E10_11 F: 5'-AGCCCCTTCCCC TGCACAGC-3', CLCN7E10_11 R: 5'-CGATGGGTGGCC CCAAGGTG-3', CLCN7E12 F: 5'-CTTCCCCTCTTGCTC TCCACT-3', CLCN7E12 R: 5'-CTATCGATGGCACGG AGAGTC-3', CLCN7E13_14 F: 5'-GGTGGTCCTTGAGTT TCAGCA-3', CLCN7E13_14 R: 5'-TAAACCCCATTCCAC CACGTC-3', CLCN7E15 F: 5'-CAGTGTCCTCCATCA GGGACT-3', CLCN7E15 R: 5'-CATTTCTCCTGGGTC CACATC-3', CLCN7E16 F: 5'-GTGTCCTCCTTGCCC TCTGT-3', CLCN7E16 R: 5'-GATCCTCCTGCCTTGGTC TCT-3', CLCN7E17 F: 5'-CTCCCCATGGGATCCTTT TAG-3', CLCN7E17 R: 5'-CCTGGTCCAGACTCCACA CAT-3', CLCN7E18_19 F: 5'-CAGCAGGGTGTACTGTGC TAGG-3', CLCN7E18_19 R: 5'-CAGAAACCCTGAGCC TACCC-3', CLCN7E20_21 F: 5'-GGGGTAGGCTCAGGG TTTCT-3', CLCN7E20_21 R: 5'-ATGGCTGCACACTCA GCTTC-3', CLCN7E22_23 F: 5'-GAGGCTGGTGTGAGC AGGTAG-3', CLCN7E22_23 R: 5'-CAGAGTCACCGA GTCCTCTCC-3', CLCN7E24_25 F: 5'-TCGGTGACTCTG TCTCCTGTG-3', CLCN7E24_25 R: 5'-ACTGCTGGG GAGCATGGTT-3'. The PCR was performed using the HotStar Taq polymerase (Takara Bio, Inc., Otsu, Japan). The thermocycling conditions were the following: 95°C for 2 min, followed by 11 cycles of 94°C for 20 sec, 64°C -0.5°C/cycle for 40 sec and 72°C for 1 min, followed by 24 cycles of 94°C for 20 sec, 58°C for 30 sec and 72°C for 1 min, the final extension was performed at 72°C for 2 min for all primer pairs except for the except for CLCN7E10_11. The thermocycling conditions used to amplify the genomic region corresponding to CLCN7E10_11 were the following: Initial denaturation at 95°C for 2 min, followed by 35 cycles of 96°C for 10 sec and 68°C for 1 min. Direct sequencing was performed using the BigDye Terminator Cycle Sequencing Ready Reaction kit, v.3.1 (Applied Biosystems; Thermo Fisher Scientific, Inc.), and the resulting PCR products were directly sequenced using an automated ABI PRISM 3130 sequencer (Applied Biosystems; Thermo Fisher Scientific, Inc.). Basic Local Alignment Search Tool (www.ncbi.nlm. nih.gov/tools/cobalt/cobalt.cgi?link_loc=BlastHomeAd) was used to perform homology analysis of the R286W, G793R, Y746D, Y99C, E313K and P470L sites in eight vertebrate species. The potential causal effects of the R286W, G793R, Y746D, Y99C, E313K and P470L missense mutations were predicted using PolyPhen-2 software (genetics.bwh.harvard. edu/pph2) (21).
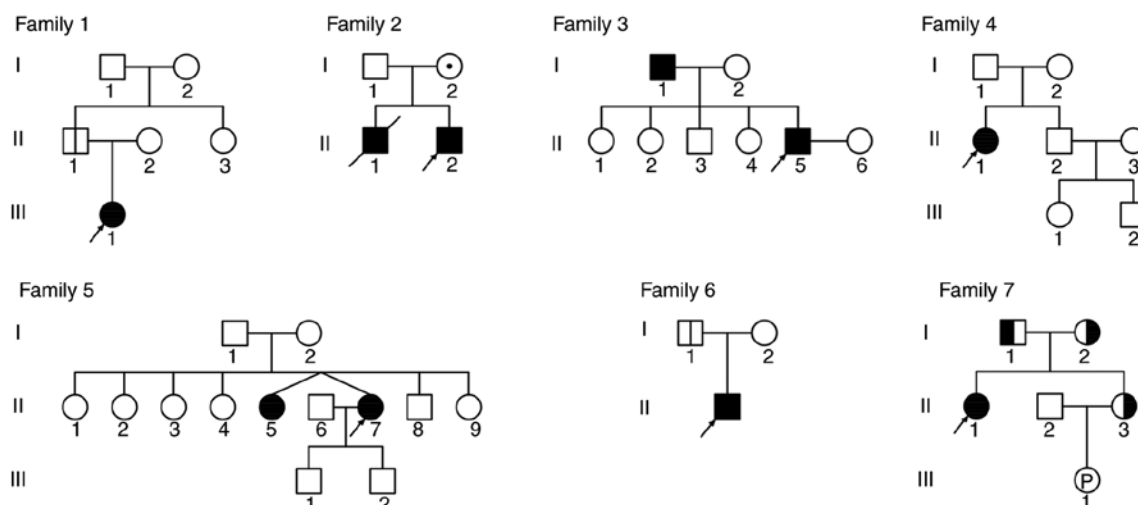
Figure 1. Pedigrees of seven families with osteopetrosis analyzed in the present study. Circles indicate females; squares indicate males. Filled black shapes indicate patients with osteopetrosis. Shapes with a trunk line indicate non-penetrant carriers of ADO-II. Shapes with a dot indicate obligate carriers of IARO. Half-black shapes indicate obligate carriers with different heterozygous mutations. Arrows indicate probands. P indicates pregnant subjects. Diagonal lines represent deceased subjects.

## Results

*Clinical manifestations of patients.* Table I presents detailed clinical parameters, biochemical results and BMDs for the patients. Fig. 2 presents radiographs from patients with ADO-II and IARO. The patients with ADO-II were diagnosed at 5-47 years old; five were male (II1 in family 1, I1 and II5 in family 3, and I1 and II1 in family 6) and four were female (III1 in family 1, II1 in family 4, and II5 and II7 in family 5). Patients with ADO-II: One patient exhibited a notably below-average height (II7 in family 5); one patient exhibited pigeon chest (II1 in family 6); three patients experienced fractures of the rib, femur, tibia and radius (II5 in family 3, II1 in family 4, II1 in family 6); one patient exhibited dental abnormalities (II5 in family 3); three patients exhibited anemia (III1 in family 1, II1 in family 4, II7 in family 5); and one patient, the proband of family 4, was diagnosed with thrombocytopenia and splenomegaly. Additionally, the proband of family 4 exhibited a visual impairment from birth.

In family 1, a 15-year-old female (proband, III1), the only daughter of nonconsanguineous parents, was born at term with a normal height and weight. The height and weight of the proband at the time of assessment were 153.3 cm and 61.0 kg, respectively. At ~1 month prior to evaluation, the proband complained of back pain. X-rays revealed an increased bone density in vertebrae, with the sandwich vertebrae sign. Laboratory data revealed an elevation in LDH levels and a minor reduction in hemoglobin (Hb) levels. Subsequently, her parents visited our department, and presented with normal BMDs.

The proband (II2) of family 2, a 24-year-old male, was the second child of nonconsanguineous parents. The proband exhibited growth retardation. The weight and height of the patient were 45 kg and 153 cm, respectively. He complained of discomfort in the abdomen and were diagnosed with osteopetrosis with anemia and hepatosplenomegaly at 3 months. He only had 20 teeth, and exhibited yellowish skin and a swollen abdomen. Additionally, he experienced a cementoma 6 years

previously; there was no deterioration. Fractures occurred in the neck of the femur when he was 4 years old and in the distal radius when he was 16 years old due to a non-violent etiology. He experienced anemia with thrombocytopenia for the majority of his life, and received a red cell suspension >3 times due to severe anemia. X-rays revealed diffuse sclerosis (Fig. 2). Laboratory data revealed increased ALP levels, and reduced Hb and PLT levels. The proband's parents exhibited normal clinical features as assessed by accessory examinations, including radiographs and BMD. The proband's older brother succumbed at the age of 3 years and was also diagnosed with osteopetrosis.

In family 3, the proband (II5), a 28-year-old male, was the youngest child of nonconsanguineous parents. The proband came to our department as a result of abnormal skeletal radiological manifestations. The weight and height of the proband were 68.0 kg and 170.5 cm, respectively. He complained of shoulder pain 10 days prior to the visit. A rib fracture with a non-violent etiology occurred during childhood. Skeletal radiography revealed an increase in bone density in the vertebrae with the sandwich vertebrae sign. Laboratory data were normal. Of the seven members of this family, including the proband's parents and other relatives, no abnormal clinical manifestations were observed, and they refused to undergo radiography or BMD assessments.

In family 4, the proband (II1), a 32-year-old female, was the first child of nonconsanguineous parents. She was born at term with normal delivery. The height and weight of the proband at the time of the examination were 153.0 cm and 67.0 kg, respectively. She was blind from birth. Fractures with a non-violent etiology occurred in the left femur twice when she was 1 and 20 years old, and in the right femur when she was 10 years old. Tinnitus and splenomegaly had developed in recent years. X-rays revealed an increase in the bone density of vertebrae with the sandwich sign and the pelvis with the bone-in-bone sign. Laboratory data revealed elevated LDH levels, and reduced Hb and PLT levels. Of the six members of the proband's family, including her parents

Table I. Clinical characteristics, biochemical results and BMD values of patients with osteopetrosis and family members.

| Family | Member | Sex | Age (years) | Height (cm) | Weight (kg) | LDH (U/l) | CK (U/l) | ALP (U/l) | Hb (g/l) | PLT (10⁹/l) | L1-4 (Z score) | FN (Z score) | TH (Z score) | Dental problem | Bone fracture | Other clinical characteristics |
|---|---|---|---|---|---|---|---|---|---|---|---|---|---|---|---|---|
| 1 | Proband | F | 15 | 153.3 | 61 | 248 | 179 | 79 | 124 | 255 | 7.7 | 4.8 | 6.6 | No | No | No |
| | Father | M | 42 | 174.7 | 92 | NA | NA | NA | NA | NA | 0.5 | 0.2 | 0.7 | No | No | No |
| 2 | Proband | M | 24 | 153.0 | 45 | 205 | 139 | 150 | 86 | 49 | 14.1 | 14.4 | 14.6 | Yes | Yes | Hepatosplenomegaly, gallstone, secondary hyperparathyroidism |
| 3 | Proband | M | 28 | 170.5 | 68 | 190 | 156 | 54 | 149 | 217 | 11.1 | 11.1 | 9.1 | Yes | Yes | No |
| 4 | Proband | F | 32 | 153.0 | 67 | 256 | 86 | 100 | 71 | 83 | 11.5 | NA | NA | No | Yes | Splenomegaly, visual impairment, tinnitus |
| 5 | Proband | F | 42 | 148.5 | 48 | NA | NA | 46 | 108 | 249 | 9.6 | 6.0 | 6.0 | No | No | Secondary hyperparathyroidism |
| 6 | Proband | M | 10 | 143.7 | 41 | 210 | 207 | 170 | 146 | 273 | 6.8 | 5.4 | 6.0 | No | Yes | Pigeon chest |
| | Father | M | 41 | 160.5 | 69 | NA | NA | 80 | 165 | 211 | 0.3 | -0.3 | -0.3 | No | No | No |
| 7 | Proband | F | 37 | 148.2 | 49 | 274 | NA | 67 | 62 | 350 | 16.9 | 17.6 | 14.1 | Yes | Yes | Visual and audile impairment, pigeon chest, cyst, arthralgia, ankylosis, deformity |
| | Father | M | 63 | 170.0 | 65 | NA | NA | NA | NA | NA | 0.4 | 0.5 | -0.3 | No | No | No |
| | Mother | F | 63 | 160.0 | 56 | NA | NA | 77 | 126 | 225 | -0.8 | -1.1 | -1.3 | No | No | No |

BMDs in probands in family 1 and 7 were measured using a Hologic DXA densitometer, and the Z scores for L1-4, FN and TH of this proband were calculated by comparison with Caucasian women. The BMDs of the other patients were measured using a Lunar DXA densitometer, and the Z scores for L1-4, FN and TH were calculated by comparison with the age-specific BMD reference values for Chinese children and adolescents. ALP, alkaline phosphate (reference range: 15-112 U/l, 75-344 U/l for children <10 years); BMD, bone mineral density; CK, creatine kinase (reference range: 21-190 U/l); DXA, dual-energy X-ray absorptiometry; FN, femoral neck BMD; Hb, hemoglobin (reference range: 130-175 g/l); L1-4, lumbar spine BMD; LDH, lactate dehydrogenase (reference range: 114-240 U/l); NA, not analyzed; PLT, platelets (reference range: 125-350x10⁹/l); TH, total hip BMD.

Figure 2. Radiology results for the patients (X-rays of skull of A, pelvis, tibia and fibula of C are taken from the proband of family 6. X-rays of vertebrae of A and C are taken from the proband of family 5. X-rays of B and D are taken from the proband of family 2). (A and C) X-rays from a patient with ADO-II. Note the generalized increase in the bone density of the skull, vertebrae, pelvis, tibia and fibula. Radiology revealed vertebral endplate thickening (the black arrow in A indicates a sandwich vertebrae sign) and typical iliac wings (the black arrow of C indicates bone-in-bone appearance). (B and D) X-rays from a patient with IARO. Note the diffuse sclerosis of the skull, vertebrae, pelvis and femur. Radiology revealed tooth destruction (white arrow in B), hip deformity (black arrow in D) and the Erlenmeyer flask deformity (white arrow in D) of the distal femur. ADO-II, autosomal dominant osteopetrosis type II; IARO, intermediate autosomal recessive osteopetrosis.

and other relatives, no abnormal clinical manifestations or BMD were observed.

In family 5, the proband (II7), a 42-year-old female, was the sixth child of nonconsanguineous parents. She came to

our department as a result of abnormal skeletal radiological manifestations. Her weight and height were 48 kg and 148.5 cm, respectively. X-rays revealed a diffuse increase in bone density with evidence of the sandwich sign in vertebrae and bone-in-bone

Table II. Summary of the findings of the molecular analysis of patients with osteopetrosis.

| Family no. | Patient/sex | Mutation site | Mutation type | Protein level | DNA level | PolyPhen-2 score | Status |
|---|---|---|---|---|---|---|---|
| 1 | III1/F | EXON9 | Missense | p.Arg286Trp | c.856C>T | 1.000 | Heterozygous |
| | II1/M | EXON9 | Missense | p.Arg286Trp | c.856C>T | 1.000 | Heterozygous |
| 2 | II2/M | EXON24 | Missense | p.Gly793Arg | c.2377G>C | 0.751 | Homozygous |
| | I2/F | EXON24 | Missense | p.Gly793Arg | c.2377G>C | 0.751 | Heterozygous |
| 3 | II5/M | INTRON22 | Putative aberrant splicing | - | c.2232-2A>G | - | Heterozygous |
| | I1/M | INTRON22 | Putative aberrant splicing | - | c.2232-2A>G | - | Heterozygous |
| 4 | II1/F | EXON10 | Missense | p.Glu313Lys | c.937G>A | 1.000 | Heterozygous |
| 5 | II7/F | EXON22 | Missense | p.Tyr746Asp | c.2236T>G | 1.000 | Heterozygous |
| 6 | II1/M | EXON3 | Missense | p.Tyr99Cys | c.296A>G | 1.000 | Heterozygous |
| | I1/M | EXON3 | Missense | p.Tyr99Cys | c.296A>G | 1.000 | Heterozygous |
| 7 | II1/F | EXON16 | Missense | p.Pro470Leu | c.1409C>T | 1.000 | Compound heterozygous |
| | | EXON7 | Insertion | p.Lys217X | c.647_648dupTG | - | |
| | I1/M | EXON16 | Missense | p.Pro470Leu | c.1409C>T | 1.000 | Heterozygous |
| | I1/F | EXON7 | Insertion | p.Lys217X | c.647_648dupTG | - | Heterozygous |
| | II3/F | EXON7 | Insertion | p.Lys217X | c.647_648dupTG | - | Heterozygous |

sign in the pelvis. Laboratory data revealed reduced Hb levels. The same signs were observed in X-rays from the proband's twin sister. The clinical manifestations, laboratory data, radiographs and BMDs of the proband's sons were normal.

In family 6, the proband (II1), a 10-year-old male, the only child of nonconsanguineous parents, was born at term with a normal length and weight. The proband's height and weight at the time of examination were 143.7 cm and 41.0 kg, respectively. He had suffered from recurrent influenza since childhood. Fractures with a non-violent etiology occurred in the left tibia when he was 3 years old and in the radius when he was 10. Pigeon chest was observed. Laboratory data revealed elevated CK levels. Their radiograph exhibited a typical appearance. The clinical manifestations, laboratory data, radiographs and BMDs of the proband's parents were normal.

The proband (II1) of family 7, a 37-year-old female, the first child of nonconsanguineous parents, experienced growth retardation. Her height and weight at the time of examination were 148.2 cm and 49.0 kg, respectively. She exhibited cysts and recurrent infections of the right knee joint during the previous 10 years. She suffered arthralgia, ankylosis and deformity of the right knee with claudication. Amblyopia of the left eye and amblyacousia of the left ear had occurred since childhood. She also experienced dental problems, including misalignment, loose teeth, tooth loss and dental cavities. A fracture of the right radius with a non-violent etiology occurred when she was 17 years old. She fainted numerous times as a result of anemia. X-rays revealed a diffuse increase in bone density. Laboratory data revealed increased LDH levels and a reduction in Hb levels. The three members of the proband's family, including her parents and sister, did not display abnormal clinical manifestations, laboratory data, radiographs or BMDs.

*Genetic analysis*. A total of one homozygous and four heterozygous missense mutations, one splice mutation and one

compound heterozygous mutation in the *CLCN7* gene were identified in the probands (Table II; Fig. 3). The heterozygous mutation (Y746D), the splice mutation (c.2232-2A>G), the homozygous mutation (G793R) and the compound heterozygous mutation (P470L and K217X) were novel. Additionally, six missense mutations, c.856C>T (R286W), c.2236T>G (Y746D), c.296A>G (Y99C), c.937G>A (E313K), c.2377G>C (G793R) and c.1409C>T (P470L), occurred at a highly conserved position, according to a comparison of the protein sequences from eight vertebrates. The missense mutations in the *CLCN7* gene (R286W, G793R, Y746D, Y99C, E313K and P470L) were predicted by PolyPhen-2 to exhibit pathogenic effects (Table II). Based on the genetic analysis, the probands in families 1, 3, 4, 5 and 6 with heterozygous mutations were diagnosed with ADO-II, whereas the proband in family 2 with the homozygous mutation and the proband in family 7 with the compound heterozygous mutation were diagnosed with IARO.

In family 1, a known heterozygous missense mutation, c.856C>T, in exon 9 of the *CLCN7* gene was identified in the proband (III1) and her father (II1), resulting in an arginine-to-tryptophan substitution at p.286. In family 2, a novel homozygous missense mutation, c.2377G>C, in exon 24 of the *CLCN7* gene was identified in the proband (II2), and a heterozygous mutation was detected in his mother (I2), resulting in a glycine-to-arginine substitution at p.793. In family 3, a novel heterozygous splice mutation, c.2232-2A>G, leading to truncated protein in intron 22 was identified in the proband (II5) and his father (I1). In family 4, a known heterozygous missense mutation, c.937G>A, in exon 10 of the *CLCN7* gene was identified in the proband (II1), resulting in a glutamate-to-lysine substitution at p.313. In family 5, the novel heterozygous missense mutation c.2236T>G in exon 22 was identified in the proband (II7) and her twin sister (II5), resulting in a tyrosine-to-aspartate substitution at p.746. In family 6, a known heterozygous missense mutation, c.296A>G, in exon 3
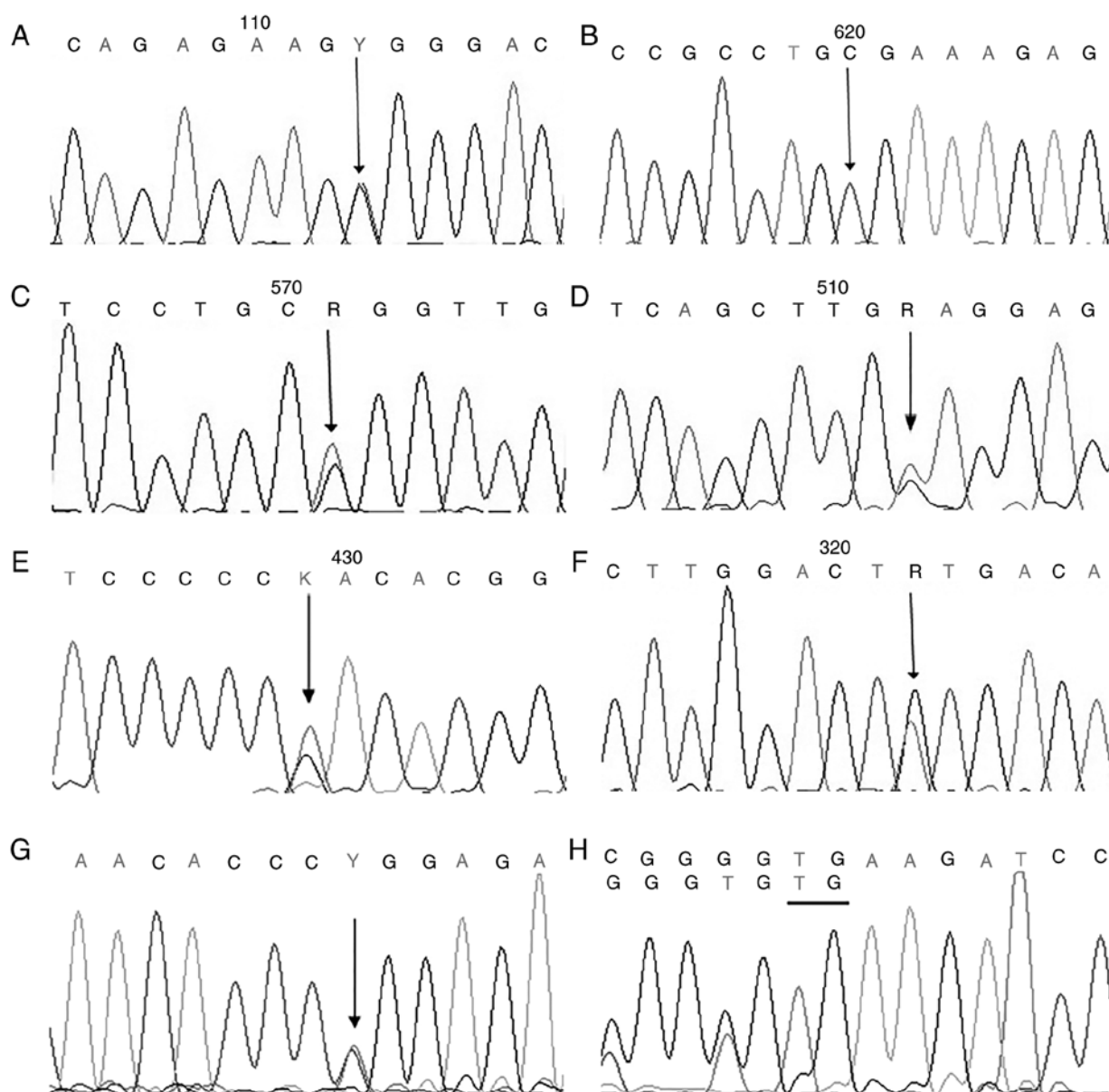
Figure 3. Analyses of mutations in the chloride channel 7 gene in patients with osteopetrosis. (A) c.856C>T mutation in exon 9. (B) c.2377G>C mutation in exon 24. (C) c.2232-2A>G mutation in intron 22. (D) c.937G>A mutation in exon 10. (E) c.2236T>G mutation in exon 22. (F) c.296A>G mutation in exon 3. (G) c.1409C>T mutation in exon 16. (H) c.647_648 dupTG mutation in exon 7.

of the *CLCN7* gene was identified in the proband (II1) and his father (I1), resulting in a tyrosine-to-cysteine substitution at p.99. In family 7, a novel insertion mutation (c.647_648 dupTG) in exon 7 was identified in the proband (II1), and her mother (I2) and sister (II3), resulting in a lysine-to-stop codon substitution at p.217 that produced a truncated protein. Additionally, a missense c.1409C>T mutation in exon 16 of the *CLCN7* gene was identified in the proband (II1) and her father (I1), resulting in a proline-to-leucine substitution at p.470. The eight mutations were not detected in the 250 healthy controls.

## Discussion

In the present study, direct sequencing of the *CLCN7* gene in the seven families revealed four heterozygous missense mutations (R286W, Y746D, Y99C and E313K), one homozygous missense mutations (G793R), one splice mutation

(c.2232-2A>G) and one compound heterozygous mutation (P470L, K217X) in the probands. The heterozygous missense mutations (R286W, Y99C and E313K) and the compound heterozygous mutation (P470L) have been reported previously (10,15,18,19). The mutations (R286W, Y746D, Y99C, G793R, E313K and P470L) all occurred at highly conserved positions among eight vertebrate species and were predicted to exert a pathogenic effect by PolyPhen-2. The *CLCN7* gene is expressed at high levels in the osteoclast ruffled membrane; ClC-7 provides the chloride conductance required for efficient proton pumping (1,4-5). CLC chloride channels are homodimers composed of two subunits, each containing 18 intramembranous α-helices, four highly conserved Cl⁻ binding sites and two cystathionine β synthase (CBS) domains (CBS1 and CBS2) located near the carboxyl terminus of the topological domain (19). Cleiren *et al* (5) first identified mutations in the *CLCN7* gene as causing ADO-II. The mutations

(R286W, Y99C, E313K and P470L) in the *CLCN7* gene have been hypothesized to be located in the intramembrane α-helices, creating a positive electrical potential to prevent the fast flux of Cl⁻ at the binding site (19). The Y746D, G793R and c.2232-2A>G mutations were hypothesized to be located in CBS2. Y746D and G793R are hypothesized to disturb protein sorting and interfere with the localization of the protein in the ruffled-border formation, which is required for normal lysosomal function and bone resorption (22,23). The novel splicing mutation (c.2232-2A>G) in the *CLCN7* gene occurred at the splice acceptor site, potentially interfering with the splicing of exon 23 with exon 24 and thereby truncating the functional domains. The novel insertion mutation (c.647_648 dupTG) in exon 7 resulted in a lysine-to-stop codon substitution at p.217, leading to the synthesis of a truncated protein. The novel *CLCN7* mutations identified in the present study may increase understanding of the spectrum of *CLCN7* mutations in this disorder.

Osteopetrosis is a rare inherited metabolic disease. ADO-II was first described by Albers-Schönberg in 1904 (5). The onset of ADO-II may occur in adulthood or childhood (16,23). Patients with ADO-II generally experience symptoms including osteosclerosis, fractures, bone pain, osteomyelitis, osteoarthritis, rickets, deafness and blindness (19). *CLCN7*-dependent IARO exhibits an autosomal recessive inheritance profile and is milder than *CLCN7*-associated ARO (1). A few cases of IARO have been previously reported (16-17,19). The onset usually occurs in the first year of life; patients frequently reach adulthood, compared with the <3-year life expectancy of patients with ARO (24).

In the present study, five families with ADO-II and two families with IARO were reported. The proband of family 4 (II1) diverged from other patients with ADO-II due to her impaired vision, increased tinnitus, bone marrow failure and splenomegaly secondary to extramedullary hematopoiesis. Waguespack et al (25) reported the rate of severe visual loss in subjects with ADO, with an overall prevalence of 19%, and a rare rate (~2%) of bone marrow failure. The proband suffered from vision loss from birth, consistent with previous reports (19,25). The mechanism by which visual loss occurs remains unclear.

In family 2, the proband (II2), a 24-year-old male from nonconsanguineous parents, was diagnosed with IARO caused by a homozygous mutation in the *CLCN7* gene, and presented with early-onset bone marrow failure (anemia and thrombocytopenia) and splenomegaly. The proband inherited one mutation from his mother; the peripheral blood DNA of his father was normal. Therefore, two possibilities existed to explain the presence of the other mutation: A germ cell mutation or germ cell mosaicism in the gonads of the proband's father, or a mutation in the fertilized egg itself. The proband's older brother (II1), who was diagnosed with osteopetrosis, succumbed at 3 years of age due to bone marrow failure and massive hepatosplenomegaly; the genotype of the brother is not known.

In family 7, the proband (II1), a 37-year-old female from nonconsanguineous parents, was diagnosed with IARO caused by a compound heterozygous mutation in the *CLCN7* gene, and presented with early-onset hearing impairments, unilateral vision impairments and pigeon chest. Notably, the P470L mutation was previously reported by Xue et al (17) to cause IARO when homozygous; however, the heterozygous mutation

P470L, inherited from the patient's father, was not predicted to cause disease. Conversely, the inheritance of an insertion mutation (resulting in a lysine-to-stop codon substitution at p.217 and truncated protein) from the patient's mother resulted in another type of IARO due to the lack of compensatory ClC-7 protein. The patient manifested notably more severe symptoms than the patients with ADO-II.

In the present study, seven symptomatic patients (including family members) with ADO-II presented classical clinical manifestations and radiographic findings. The father (II1) in family 1 and the father (I1) in family 6 were unaffected gene carriers with normal biochemical measurements, radiographs and BMDs. The penetrance of ADO-II was ~66%, with a highly variable phenotype. The association between genotype and phenotype was difficult to determine in the present study. Modifier genes, DNA methylation or intrinsic osteoclast factors may serve roles in the manifestation of this disease. Further studies should be performed to determine the mechanism of incomplete penetrance.

There were a number of limitations in our study. The relatively small sample size, including only two cases of IARO, were insufficient to characterize all the properties of *CLCN7*-dependent osteopetrosis or determine phenotype-genotype associations. In addition, investigations into the mechanisms underlying the effects of these novel mutations were not determined, and further in-depth research is required.

In conclusion, various mutations (R286W, Y746D, Y99C, G793R, E313K, c.2232-2A>G, P470L and K217X) in the *CLCN7* gene were identified in six patients (the probands in family 1, 2, 3, 5, 6, 7) with familial osteopetrosis and one patient (the proband in family 4) with sporadic osteopetrosis. Furthermore, the phenotypes of patients with ADO-II and IARO were characterized. The findings from the present study increase the spectrum of reported *CLCN7* gene mutations and improve the present understanding of osteopetrosis. Additionally, it may aid further studies aiming to dissect the heterogeneity of ADO-II and IARO.

## Availability of data and materials

All data generated or analyzed during the present study are included in this published article.

## Authors' contributions

ZZ and HY designed and conceived the present study and analyzed the genetic test results. LL and SL analyzed the

clinical information, analyzed the genetic test results and drafted the manuscript. CW collected and analyzed data. All authors read and approved the final manuscript.

## Ethics approval and consent to participate

The present study was approved by the Ethics Committee of the Shanghai Jiao Tong University Affiliated Sixth People's Hospital. All participants provided written informed consent.

## Patient consent for publication

All patients within this study provided consent for the publication of their data.

## Competing interests

The authors declare that they have no competing interests.

## References

1. Del Fattore A, Cappariello A and Teti A: Genetics, pathogenesis and complications of osteopetrosis. Bone 42: 19-29, 2008.
2. Coudert AE, de Vernejoul MC, Muraca M and Del Fattore A: Osteopetrosis and its relevance for the discovery of new functions associated with the skeleton. Int J Endocrinol 2015: 372156, 2015.
3. Palagano E, Blair HC, Pangrazio A, Tourkova I, Strina D, Angius A, Cuccuru G, Oppo M, Uva P, Van Hul W, et al: Buried in the middle but guilty: Intronic mutations in the TCIRG1 gene cause human autosomal recessive osteopetrosis. J Bone Miner Res 30: 1814-1821, 2015.
4. Tolar J, Teitelbaum S and Orchard P: Osteopetrosis. N Engl J Med 351: 2839-2849, 2004.
5. Cleiren E, Bénichou O, Van Hul E, Gram J, Bollerslev J, Singer FR, Beaverson K, Aledo A, Whyte MP, Yoneyama T, et al: Albers-Schönberg disease (autosomal dominant osteopetrosis, type II) results from mutations in the ClCN7 chloride channel gene. Hum Mol Genet 10: 2861-2867, 2001.
6. Bénichou O, Cleiren E, Gram J, Bollerslev J, de Vernejoul MC and Van Hul W: Mapping of autosomal dominant osteopetrosis type II (Albers-Schönberg disease) to chromosome 16p13.3. Am J Hum Genet 69: 647-654, 2001.
7. Cappariello A, Maurizi A, Veeriah V and Teti A: Reprint of: The great beauty of the osteoclast. Arch Biochem Biophys 561: 13-21, 2014.
8. Teti A: Bone development: Overview of bone cells and signaling. Curr Osteoporos Rep 9: 264-273, 2011.
9. Kuroyanagi Y, Kawasaki H, Noda Y, Ohmachi T, Sekiya S, Yoshimura K, Ohe C, Michigami T, Ozono K and Kaneko K: A fatal case of infantile malignant osteopetrosis complicated by pulmonary arterial hypertension after hematopoietic stem cell transplantation. Tohoku J Exp Med 234: 309-312, 2014.
10. Zheng H, Shao C, Zheng Y, He JW, Fu WZ, Wang C and Zhang ZL: Two novel mutations of CLCN7 gene in Chinese families with autosomal dominant osteopetrosis (type II). J Bone Miner Metab 34: 440-446, 2016.
11. Deng H, He D, Rong P, Xu H, Yuan L, Li L, Lu Q and Guo Y: Novel CLCN7 mutation identified in a Han Chinese family with autosomal dominant osteopetrosis-2. Mol Pain 12: 1744806916652628, 2016.
12. Faden MA, Krakow D, Ezgu F, Rimoin DL and Lachman RS: The Erlenmeyer flask bone deformity in the skeletal dysplasias. Am J Med Genet A 149A: 1334-1345, 2009.
13. Boudin E and Van Hul W: Sclerosing bone dysplasias. Best Pract Res Clin Endocrinol Metab 32: 707-723, 2018.
14. Zhang ZL, He JW, Zhang H, Hu WW, Fu WZ, Gu JM, Yu JB, Gao G, Hu YQ, Li M and Liu YJ: Identification of the CLCN7 gene mutations in two Chinese families with autosomal dominant osteopetrosis (type II). J Bone Miner Metab 27: 444-451, 2009.
15. Wang C, Zhang H, He JW, Gu JM, Hu WW, Hu YQ, Li M, Liu YJ, Fu WZ, Yue H, et al: The virulence gene and clinical phenotypes of osteopetrosis in the Chinese population: Six novel mutations of the CLCN7 gene in twelve osteopetrosis families. J Bone Miner Metab 30: 338-348, 2012.
16. Zhang X, Wei Z, He J, Wang C and Zhang Z: Novel mutations of CLCN7 cause autosomal dominant osteopetrosis type II (ADOII) and intermediate autosomal recessive osteopetrosis (ARO) in seven Chinese families. Postgrad Med 129: 934-942, 2017.
17. Xue Y, Wang W, Mao T and Duan X: Report of two Chinese patients suffering from CLCN7-related osteopetrosis and root dysplasia. J Craniomaxillofac Surg 40: 416-420, 2012.
18. Zeng B, Li R, Hu Y, Hu B, Zhao Q, Liu H, Yuan P and Wang Y: A novel mutation and a known mutation in the CLCN7 gene associated with relatively stable infantile malignant osteopetrosis in a Chinese patient. Gene 576: 176-181, 2016.
19. Pang Q, Chi Y, Zhao Z, Xing X, Li M, Wang O, Jiang Y, Liao R, Sun Y, Dong J and Xia W: Novel mutations of CLCN7 cause autosomal dominant osteopetrosis type II (ADO-II) and intermediate autosomal recessive osteopetrosis (IARO) in Chinese patients. Osteoporos Int 27: 1047-1055, 2016.
20. Zheng H, Zhang Z, He JW, Fu WZ, Wang C and Zhang ZL: Identification of two novel CLCN7 gene mutations in three Chinese families with autosomal dominant osteopetrosis type II. Joint Bone Spine 81: 188-189, 2014.
21. Adzhubei IA, Schmidt S, Peshkin L, Ramensky VE, Gerasimova A, Bork P, Kondrashov AS and Sunyaev SR: A method and server for predicting damaging missense mutations. Nat Methods 7: 248-249, 2010.
22. Lange PF, Wartosch L, Jentsch TJ and Fuhrmann JC: ClC-7 requires Ostm1 as a beta-subunit to support bone resorption and lysosomal function. Nature 440: 220-223, 2006.
23. Sobacchi C, Schulz A, Coxon FP, Villa A and Helfrich MH: Osteopetrosis: Genetics, treatment and new insights into osteoclast function. Nat Rev Endocrinol 9: 522-536, 2013.
24. Villa A, Guerrini MM, Cassani B, Pangrazio A and Sobacchi C: Infantile malignant, autosomal recessive osteopetrosis: The rich and the poor. Calcif Tissue Int 84: 1-12, 2009.
25. Waguespack SG, Hui SL, Dimeglio LA and Econs MJ: Autosomal dominant osteopetrosis: Clinical severity and natural history of 94 subjects with a chloride channel 7 gene mutation. J Clin Endocrinol Metab 92: 771-778, 2007.